

## BULL SPERM RHEOTAXIS AND KINEMATICS IN MICROFLUIDIC CHANNELS WITH DIFFERENT HEIGHTS

HAITHAM A. MOFADEL<sup>1</sup>; HASSAN A. HUSSIEN<sup>2</sup>; AHMED M.R. FATH EL-BAB<sup>3</sup> and<sup>4</sup> TAYMOUR M. EL-SHERRY

<sup>1</sup> Department of Theriogenology, Faculty of Veterinary Medicine, Assiut University, Assiut 71526, Egypt. [Haitham\\_Mofadel@aun.edu.eg](mailto:Haitham_Mofadel@aun.edu.eg) (\*)

<sup>2</sup> Department of Theriogenology, Faculty of Veterinary Medicine, Assiut University, Assiut 71526, Egypt. [hassan.hussien@vet.au.edu.eg](mailto:hassan.hussien@vet.au.edu.eg)

<sup>3</sup> Mechatronics and Robotics Department, Egypt-Japan University of Science and Technology (E-JUST), Alexandria 21934, Egypt [ahmed.rashad@ejust.edu.eg](mailto:ahmed.rashad@ejust.edu.eg)

<sup>4</sup> Department of Theriogenology, Faculty of Veterinary Medicine, Assiut University, Assiut 71526, Egypt [timour.ibrahim@vet.au.edu.eg](mailto:timour.ibrahim@vet.au.edu.eg)

**Received:** 1 August 2023; **Accepted:** 20 September 2023

---

### ABSTRACT

Recently, microfluidics has attracted a lot of attention in reproduction due to its ability to simulate the natural environment inside the female reproductive tract and its ability to separate high-quality sperm cells using rheotaxis as a selection mechanism. Positive rheotaxis refers to the ability of the sperm to direct itself and swim against the liquid current during the fertilization journey. In this study, we investigated the effects of various microchannel heights on sperm positive rheotaxis (PR) and sperm kinematics. We used two microchannels with the same width (200 $\mu$ m) and different heights (channel 1= 20  $\mu$ m height and channel 2= 100  $\mu$ m height). Sperm samples were obtained from two bulls with known fertility and analyzed using CASA. The results showed that PR and all sperm kinematics (VCL, VSL, VAP, and BCF), except linearity, were significantly higher in microchannel 2 with a greater height (100  $\mu$ m) than in microchannel 1 with a lower height (20  $\mu$ m). Our findings indicate that PR percentage and sperm kinematic values in microfluidic platforms depend mainly on microchannel dimensions, which have a direct influence on the velocity profile inside the channel. These results could be useful for the development of microfluidic devices used for sperm separation and selection in the future.

**Key words:** Microchannel dimension, sperm rheotaxis; cryopreserved semen; CASA parameters; cattle.

---

### INTRODUCTION

There is a crucial need to improve the efficiency and sustainability of food-

producing animals in the face of the ever-growing world population. Therefore, improving the fertility of livestock, especially cattle, is essential for overcoming this problem. This can be achieved by a better understanding of the mechanisms and challenges of reproductive technologies, which are important for improving the livestock industry (Medeiros *et al.*, 2002). In

---

*Corresponding author:* Haitham A. Mofadel

*E-mail address:* [Haitham\\_Mofadel@aun.edu.eg](mailto:Haitham_Mofadel@aun.edu.eg)

*Present address:* Department of Theriogenology, Faculty of Veterinary Medicine, Assiut University, Assiut 71526, Egypt.

most mammals, millions or even billions of sperms are inseminated during coitus, but only thousands of them can reach the fallopian tube; overall, less than 100 sperm cells can make it to the site of fertilization (Suarez, 2002). The reduction in sperm number is due to several selection mechanisms by which sperm cells must pass during their journey to the oocyte. These selection mechanisms are very important in removing damaged and immature spermatozoa (Suarez, 2006), and simultaneously obtaining fertilizing ability. Therefore, only functionally normal spermatozoa can reach the fertilization site in the oviduct (Morrell and Rodriguez-Martinez, 2011). The challenges of the female reproductive tract include the acidic PH of the vagina (O'Hanlon *et al.*, 2013), thick mucus in some parts of the female reproductive tract (Suarez *et al.*, 1997), immune responses to sperm cells (Wigby *et al.*, 2019), the long journey to the oocyte, the small size of the oocyte as a target, the folds and bends along the genital tract (Kölle, 2015; Suarez and Pacey, 2006; Yániz *et al.*, 2000), and the direction of the fluid current towards the vagina (June Mullins and Saacke, 1989). In the female genital tract, sperm are guided by different mechanisms for successful arrival to the oocyte, including chemotaxis, which means the attraction of sperm to the oocyte, as oocytes secrete chemical agents such as (peptides, amino acids, lipids, and sulfated steroids, which cause uneven beating of sperm flagellum leading to movement of sperm towards the oocyte (Chang and Suarez, 2010; Eisenbach and Giojalas, 2006), Thermotaxis refers to the swimming of sperm cells in response to a temperature gradient (Bahat *et al.*, 2003) and recently rheotaxis, in which cells move against the flow. Rheotaxis is believed to be a long-range sperm-guidance mechanism (El-sherry *et al.*, 2017; Ishikawa *et al.*, 2016; Mathijssen *et al.*, 2016; Zhang *et al.*, 2016). Sperm rheotaxis is also considered the major sperm guidance mechanism as 80-84 % of bull spermatozoa (El-Sherry *et al.*, 2014) and about 49% of human sperm show rheotaxis, whereas chemotaxis is short range guidance

mechanism that only guides sperm within few millimeters to enter the oocyte (Eisenbach, 1999; Pérez-Cerezales *et al.*, 2015) and only 10% of sperm cells in mouse (Eisenbach, 1999; Giojalas and Roasio, 1998; Nishina *et al.*, 2019) and 2-12% of human sperms show chemotaxis (Cohen-Dayag *et al.*, 1994; Eisenbach, 1999). At the same time only 3-5% of human spermatozoa display thermotaxis (Bahat *et al.*, 2003). Sperm rheotaxis has proven to be a great tool for the selection of high-quality sperm cells (De Martin *et al.*, 2017; Rappa *et al.*, 2018; Romero-Aguirregomez-corta *et al.*, 2021; Sarbandi *et al.*, 2021; Sharma *et al.*, 2022) which in turn will help overcome infertility problems and facilitate the development of other assisted reproductive technologies (ART). Although sperm rheotaxis is known as sperm guidance (El-sherry *et al.*, 2017; Ishikawa *et al.*, 2016; Mathijssen *et al.*, 2016; Zhang *et al.*, 2016) and selection mechanism (De Martin *et al.*, 2017; Rappa *et al.*, 2018; Romero-Aguirregomez-corta *et al.*, 2021; Sarbandi *et al.*, 2021; Sharma *et al.*, 2022), little is known about the effect of different microchannel dimensions on sperm rheotaxis. In this study, we designed an experiment to investigate the impact of different microchannel heights on sperm rheotaxis percentage and sperm kinematics.

## MATERIALS AND METHODS

### 1 Reagents

All chemicals were purchased from Elgomhoria Pharmaceuticals (Cairo, Egypt). Microchannel fabrication materials were obtained as follows: diacetone alcohol purchased from Sigma Aldrich, Steinheim, Germany, glass wafers from Howard Glass, Worcester, MA, SU-8-25 negative resist from MicroChem, Newton, CA, and polydimethylsiloxane PDMS from Syllgard-184, Dow Corning, Midland, MI.

### 2 Semen samples

Commercial frozen semen straws (n = 14) were obtained from the Veterinary Medicine Directorate in the Assiut Governorate from

two fertile bulls (seven straws per bull obtained from 3 ejaculates). Semen in straws was thawed in a water bath at 37 °C for 30 s and then diluted three times with sodium citrate due to the presence of glycerol, which prevented flow generation inside the microchannel. After dilution, the straw was divided into two equal halves for further analysis using two microchannels of the same width (200µm) and different heights (channel 1 = 20 µm height and channel 2 = 100 µm height). Final sperm concentration inside both of microchannels was around  $15 \times 10^6$  sperm/ml.

### 3 Microfluidic Device fabrication

#### 3.1 PDMS microchannels (microchannel 1)

Soft lithography was used for the fabrication of PDMS microchannels, as extensively explained by (Duffy *et al.*, 1998). The method will be described here briefly. In the beginning, a high-resolution printer was used to print the transparent mask that holding the microchannel design (Prismatic, Cairo, Egypt and Pacific Arts and Design, Markham, ON). Wafers were used as a substrate for masters. After cleaning wafers in acetone, isopropyl alcohol, and DI water they were covered by a 20-µm- Thick layer of SU8-25 through using a spin coating (3,000 rpm, 1 min). After that, the SU-8 layer was soft-baked at 65°C for 2 min, and at 95°C for 10 min) and exposed to ultraviolet light for 50 s. To cross-link the exposed SU-8 layer, the post-exposure bake was accomplished at 65°C for 1 min; and at 95°C for 4 min, then it was developed in diacetone alcohol for 6.5 min. For further hardening of the SU-8 layer, the wafers were hard-baked at 200°C for 15 min.

To make Polydimethylsiloxane (PDMS) a Monomer and curing agent were mixed at a ratio of 10:1 according to weight respectively, after that it was degassed using a vacuum desiccator. Finally, it was poured on the SU8 master. PDMS was dried in an oven at 120°C for 30 minutes, then the

microchannels were cut out of the master by peeling. Microchannels were perforated at the inlet and the outlet to make a place for tubing connections. To permanently bond the PDMS microchannel with a glass slide (microscope glass slide) we used a movable corona treater (Electro-Technic Products, Chicago, IL) (Haubert *et al.*, 2006). The microchannel dimensions used in this study were 200 µm × 20 µm (W×H). Figure 1(a) shows the picture of the microchannel 1 (PDMS channel with 20 µm height) used in this study.

#### 3.2 PMMA Lithography craved microchannel (microchannel 2).

The microchannel consists of 2 parts made from PMMA, the proximal part holds the inlet ports while the distal one bears the craved microchannel, as shown in Fig1 (b). Direct write laser machining technique was used in the manufacture of this PMMA channel. For microchannel fabrication the following were used: VLS3.5 UNEVERSAL LASER SYSTEMS along with a 30-Watt CO2 laser tube and laser beam of 100 µm diameter. The best engraving was reached through regulating the speed of engraving to 25 mm s<sup>-1</sup> (10%) laser head translation speed and adjusting the power of laser beam to 5-Watt (6%) laser beam power so we can get less roughness at the lowest dimensions. The microchannel profile is a Gaussian shape as shown in Fig 2 (c).

Bonding the proximal and the distal part of the PMMA microchannel was done through the thermocompression method along with acetic acid at 115°C and 1 N for 7 minutes. Heating with acetic acid resulted in improved both bonding at lower temperature and bonding time (Nasser *et al.*, 2019). The dimensions of the PMMA microchannel used in this study were 200 µm × 100 µm (W×H). Figure 1(d) shows the picture of microchannel 2 (PMMA channel with 100 µm height) used in this study.

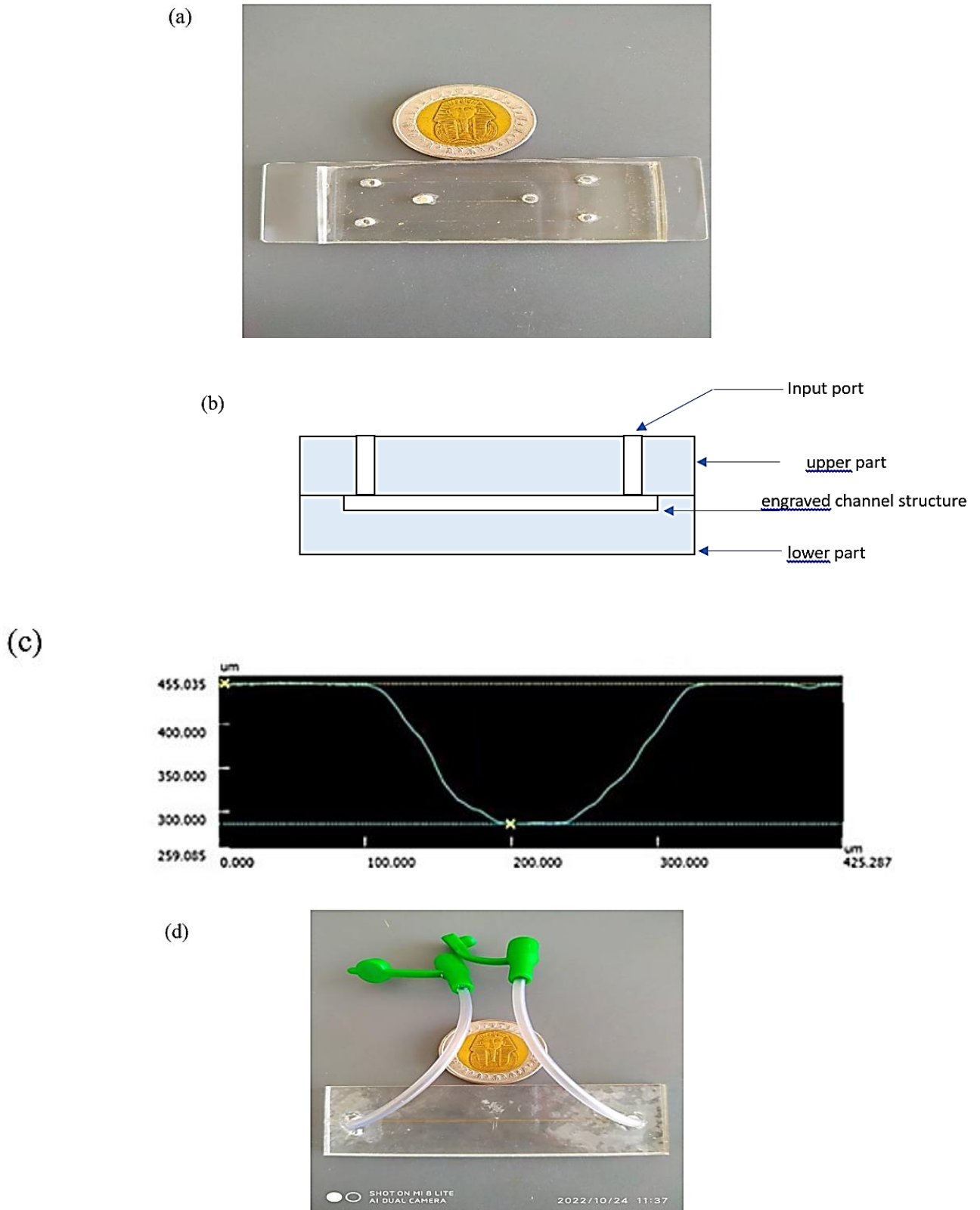


**Figure 1:** (a) Picture microchannel 1(PDMS channel with 20  $\mu\text{m}$  height) used in the present study. (b) Chip schematic drawing for microchannel 2. (c) microchannel 2 profile. (d) Picture of microchannel 2 (PMMA channel with 100  $\mu\text{m}$  height) used in the present study.

## 2.4 Flow generation

The liquid current was generated inside the microchannel by using hydrostatic pressure as the liquid level kept higher at the inlet of the channel than that of the outlet by height different  $\Delta h$ . This method of hydrostatic flow generation has proved to be a simple and cheap method for flow generation inside microchannels and doesn't have pulsating flow problems which is common with syringe pumps (Moscovici *et al.*, 2010). Darcy–Weisbach equation was used to calculate the average flow velocity inside the microchannels (Munson *et al.*, 2002).

$$V_{av} = \frac{(2\rho g Dh \Delta h)}{C \mu L}$$

In the previous equation  $\rho$  represents the liquid density,  $g$  is the gravitational acceleration,  $Dh$  represents the hydraulic diameter of the microchannel,  $\Delta h$  represents the height difference between the inlet and the outlet of the channel,  $C = f \times \text{Re}$ , while  $\mu$  is the liquid viscosity and  $L$  represents the length of the microchannel (Munson *et al.*, 2002). Equation (2) was used to calculate the velocity profile (velocity distribution) inside the microchannels. This equation is used for channels with an aspect ratio less than 0.5 (SHAH and AL, 1978)

$$(2) \frac{V}{V_{av}} = \left(\frac{m+1}{m}\right) \left(\frac{n+1}{n}\right) \left[1 - \left(\frac{y}{b}\right)^n\right] \left[1 - \left(\frac{z}{a}\right)^m\right]$$

In equation 2  $V$  represents the liquid flow velocity at any site inside the microchannel. where  $a$ , and  $b$  are the microchannel width and height, respectively., on the other hand  $y$  and  $z$  represent the coordinates (measured from the centreline) of any location in the microchannel. So, we need to calculate  $V$ , and  $m$  and  $n$  are numerical parameters that depend on microchannel aspect ratio,  $\alpha = b/a$  as shown by equations (3) and (4).

$$(3) \quad m = 1.7 + 0.5\alpha^{-1.4}$$

$$(4) \quad \begin{cases} n = 2 \\ n = 2 + 0.3(\alpha - 1/3) \end{cases} \begin{cases} \alpha < \frac{1}{3} \\ \alpha \geq \frac{1}{3} \end{cases}$$

The average liquid velocity in this experiment was kept at  $32 \mu\text{m/s}$

## 5 sperm rheotaxis and sperm kinematics analyses using CASA.

A home-made computer-assisted sperm analysis CASA was used to evaluate positive rheotaxis and all sperm kinematic values (Department of Mechanical Engineering, Faculty of Engineering, Assiut University, Egypt; the plugin can be downloaded from the following [URL:http://www.assiutmicrofluidics.com/research/casa](http://www.assiutmicrofluidics.com/research/casa)) (Elsayed *et al.*, 2015). All videos were recorded by a  $40 \times$  objectives lens of Optika XDS-3 inverted microscope with phase contrast attached to a camera (Tucsen ISH1000) regulated at 30 frames/s. All recorded videos were analyzed through the CASA system that was mentioned previously. In addition, to sperm positive rheotaxis two sets of sperm parameters were determined: velocity parameters such as curvilinear velocity (VCL,  $\mu\text{m/s}$ ), straight-line velocity (VSL,  $\mu\text{m/s}$ ) and average path velocity (VAP,  $\mu\text{m/s}$ ). progression parameters such as linearity (LIN= VSL/VCL) and beat cross frequency (BCF, Hz).

## Statistics

All data for sperm rheotaxis and sperm kinematics were analyzed using one way analysis of variance (ANOVA) followed by Tukey multiple comparison test to determine the differences between the means of the two microchannels. Statistical analysis was performed using Graph Pad Prism version 8.0.0 for Windows, Graph Pad Software, San Diego, California, USA, [www.graphpad.com](http://www.graphpad.com)".

## RESULTS

### 1. Sperm rheotaxis and kinematics in 2 different height microchannels

Videos were recorded for sperm cell motion inside two microchannels of two different heights (microchannel 1 = 20  $\mu\text{m}$  height and microchannel 2 = 100  $\mu\text{m}$  height) using CASA. The results of all analyzed data for sperm rheotaxis and sperm kinematics

showed significant differences. The percentages of positive rheotaxis, VCL, VSL, VAP, and BCF were significantly higher in microchannel 2 than in microchannel 1, as shown in Table 1, FIG2(a, b, c, d, and f). LIN(VSL/VCL) was the only CASA parameter that was found to be significantly higher in microchannel 1 than in microchannel 2, as shown in Table 1, FIG2(e).

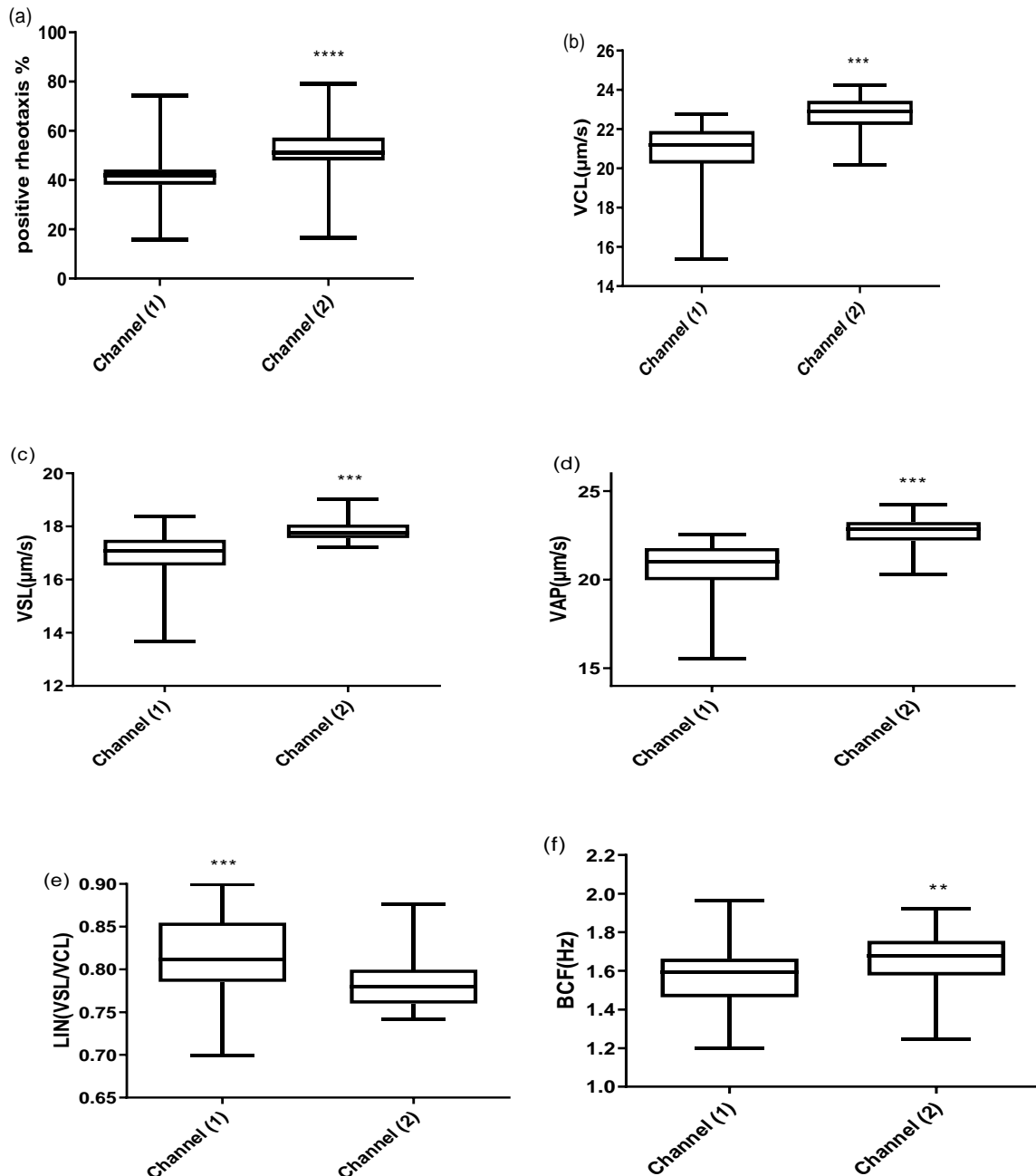


**Figure 2:** (a) Percent of positive rheotaxis. (b,c,d,e,f) CASA parameters (velocity and progression parameters) of sperm cells in microchannel 1 and 2. Data represented in mean  $\pm$  SEM. Asterisk \* indicate significance at  $P < 0.01$ .

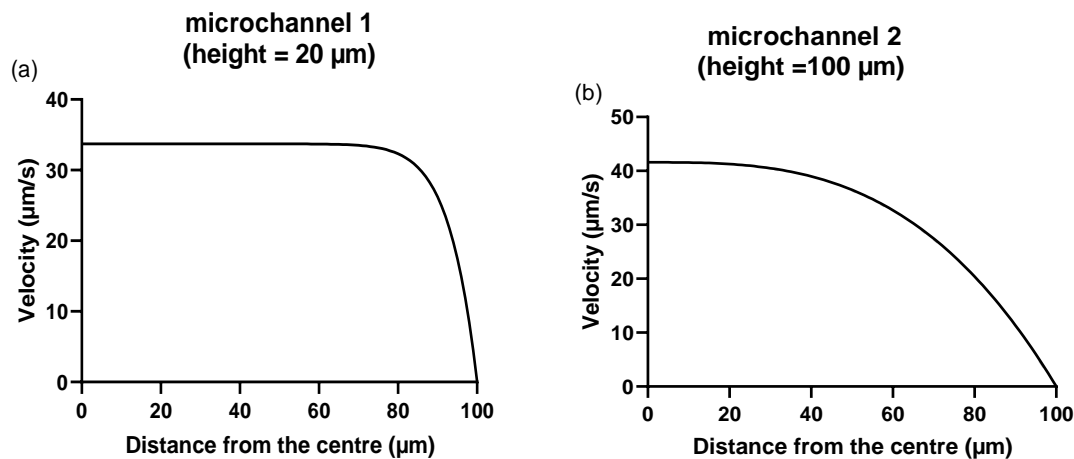


**Figure 3:** flow velocity profile inside microchannels. (a) microchannel 1, (b) microchannel 2

**Table 1:** Sperm number (N), the positive rheotaxis % (PR), curvilinear velocity (VCL), straight line velocity (VSL), average path velocity (VAP), linearity (LIN=VSL/VCL) and Beat/cross-frequency (BCF) in microchannels with two different heights. The asterisk \* indicates significance at  $P < 0.01$ .

Microchannel	N	PR%	VCL ( $\mu\text{m/s}$ )	VSL ( $\mu\text{m/s}$ )	VAP ( $\mu\text{m/s}$ )	LIN (VSL/VCL)	BCF(Hz)
<b>Microchannel1 (20<math>\mu\text{m}</math> height)</b>	37217	41.97 $\pm$ 1.2	20.85 $\pm$ 0.19	16.92 $\pm$ 0.1	20.7 $\pm$ 0.19	0.8 $\pm$ 0.006*	1.58 $\pm$ 0.02
<b>Microchanne2 (100<math>\mu\text{m}</math> heigh)</b>	40160	54.45 $\pm$ 1.7*	22.77 $\pm$ 0.12*	17.8 $\pm$ 0.05*	22.7 $\pm$ 0.1*	0.78 $\pm$ 0.004	1.66 $\pm$ 0.02*
<b>P value</b>		<0.0001	<0.0001	<0.0001	<0.0001	<0.0001	< 0.01

## DISCUSSION

Our results showed that positive sperm rheotaxis was significantly higher in Microchannel 2 (100  $\mu\text{m}$  height) than in Microchannel 1 (20  $\mu\text{m}$  height). El-Sherry *et al.*, (2014) reported that sperm cells showed a higher percentage of positive rheotaxis in microchannels with the larger width (200  $\mu\text{m}$ ) than the other channel with the smaller width (50  $\mu\text{m}$ ) at a flow velocity of 33  $\mu\text{m s}^{-1}$ . However, when the flow speed was increased to 67 or 101  $\mu\text{m s}^{-1}$ , the PR was significantly higher in the 50  $\mu\text{m}$  wide microchannel than in the 200  $\mu\text{m}$  wide microchannel. These results were explained in terms of the flow velocity distribution inside the microchannel (El-Sherry *et al.*, 2014). The explanation of the current study results also depends on the distribution of flow velocity inside the microchannel. Our velocity profile results revealed that the velocity profile inside microchannel 1 (20  $\mu\text{m}$  height) was almost flat, with a maximum velocity similar to the average

flow velocity. Fig 3 (a). However, the velocity profile inside microchannel 2 (100  $\mu\text{m}$  height) was different, as approximately 60% of the sperm in the channel were exposed to a considerably higher velocity than the average flow velocity Fig 3(b). Considering that sperm-positive rheotaxis is positively correlated with flow speed (El-Sherry *et al.*, 2014). Thus, the increase in the flow velocity inside microchannel 2 led to an increase in the PR % in microchannel 2 compared to that in microchannel 1. In contrast, a recent study showed that as the microchannel dimensions decreased, the PR% increased (Nishina *et al.*, 2019). This may be because cylindrical microchannels with different dimensions were used in this study, which resulted in different distributions of flow velocity as well as fluid shear stress inside the microchannel. While in the previous (El-Sherry *et al.*, 2014) and in the current study, rectangular channels were used. In two other studies, the used channels had a larger diameter than that used in our experiment. As one of them used a glass micropipette on 35 mm petri dish and the height of the fluid was 1,000  $\mu\text{m}$ . The

rheotaxis percentage was 49% (Zhang *et al.*, 2016). In the other experiment, they used a capillary tube with 1000  $\mu\text{m}$  width and 50  $\mu\text{m}$  height and the rheotaxis percentage was 51% (Miki and Clapham, 2013). On comparison of these experiments with each other, it appears that the percentage of positive rheotaxis increased as the microchannel diameter decreased. These results could be due to the greater height of these channels that result in lower shear rate and stress near the walls of the channel (Miki and Clapham, 2013; Zhang *et al.*, 2016).

In the present study, we compared the sperm kinematics of positive rheotactic sperms in these two microchannels with different heights, and the results revealed that microchannel 2 had significantly higher sperm kinematics (VCL, VSL, VAP, and BCF) than microchannel 1. On the other hand, the linearity was significantly higher in microchannel 1 than in microchannel 2. Sperm kinematics results could also be clarified in terms of velocity. It has been reported that sperm swimming velocity increases as the flow velocity increases, so sperm can keep swimming against the liquid current until a certain limit of flow velocity (134  $\mu\text{m s}^{-1}$ ) (El-Sherry *et al.*, 2014). In the present study, a large number of sperm cells (60 %) were exposed to flow velocities higher than the average inside microchannel 2 than those inside microchannel 1, as explained previously. This difference in flow speed results in an increase in velocity parameters (VCL, VSL, and VAP) and BCF of sperm cells inside channel 2 compared to those present in channel 1 (so they can keep swimming against the flow). Linearity was the only parameter that was significantly higher inside Channel 1 than in Channel 2. The increase in linearity was probably due to the inability of sperm to be freely movable within channel 1 because of the lower height (20  $\mu\text{m}$ ), which resulted in lower VCL and thus higher linearity as  $\text{linearity} = \text{VSL}/\text{VCL}$ . The type of chamber used for semen analysis by CASA was found to have a tremendous effect on sperm motility and sperm kinetics (Contri *et al.*, 2010). Difference in CASA parameters results between the used chambers was traced to fluid dynamics and

chamber depth and shape for example chamber shape was rectangular in the Leja and round in the Makler (Contri *et al.*, 2010). In goat, sperm velocity parameters and progressive motility were found to be higher in 20  $\mu\text{m}$  than 10  $\mu\text{m}$  depth capillary loading chamber (Del Gallego *et al.*, 2017). Furthermore, it was reported that sperm kinematics obtained from 100  $\mu\text{m}$  depth chamber were significantly higher than those obtained from chambers with lower depth (10 – 20  $\mu\text{m}$ ) (Soler *et al.*, 2018). Although the results of the previous studies (Contri *et al.*, 2010; Del Gallego *et al.*, 2017; Soler *et al.*, 2018) came from counting chambers used for CASA analysis and not microchannels with fluid current as in the present study, they still prove that the diameter and shape of sperm analysis container have a direct influence on sperm motility and kinematics and come in an agreement with our results.

## CONCLUSIONS

From the current study, we can conclude that the dimensions of rectangular microchannels (height) have a significant and direct effect on the percentage of sperm-positive rheotaxis and even on other CASA parameters. This information can be used in the development of microfluidic devices for assisted reproductive technologies, such as sperm selection and in vitro fertilization.

## Author contributions

The work was divided equally among the authors. Haitham A. Mofadel and Taymour M. El-Sherry. including research study, statistical analysis, and writing of the paper. Ahmed M.R. Fath El-Bab fabricated and provided the microchannels used in the study. This research is part of Haitham A. Mofadel's master thesis and under the supervision of professors Taymour M. El-Sherry and Hassan A. Hussien.

## Funding

Funding was offered by Assiut University.

### Competing interests

The authors declare that there is no competing interest.

### REFERENCES

- Bahat, Tur-Kaspa, Gakamsky, Giojalas, Breitbart and Eisenbach (2003)*: Thermotaxis of mammalian sperm cells: a potential navigation mechanism in the female genital tract. *Nature medicine*, 9(2), 149-150.
- Chang and Suarez (2010)*: Rethinking the relationship between hyperactivation and chemotaxis in mammalian sperm. *Biology of reproduction*, 83(4), 507-513.
- Cohen-Dayag, Ralt, Tur-Kaspa, Manor, Makler, Dor, Eisenbach (1994)*: Sequential acquisition of chemotactic responsiveness by human spermatozoa. *Biology of reproduction*, 50(4), 786-790.
- Contri, Valorz; Faustini, Wegher and Carluccio (2010)*: Effect of semen preparation on casa motility results in cryopreserved bull spermatozoa. *Theriogenology*, 74(3), 424-435.
- De Martin, Cocuzza, Tiseo, Wood, Miranda, Monteleone and Baracat (2017)*: Positive rheotaxis extended drop: a one-step procedure to select and recover sperm with mature chromatin for intracytoplasmic sperm injection. *Journal of assisted reproduction and genetics*, 34, 1699-1708.
- Del Gallego, Sadeghi, Blasco, Soler, Yániz, and Silvestre (2017)*: Effect of chamber characteristics, loading and analysis time on motility and kinetic variables analysed with the CASA-mot system in goat sperm. *Animal Reproduction Science*, 177, 97-104.
- Duffy, McDonald, Schueller and Whitesides (1998)*: Rapid prototyping of microfluidic systems in poly (dimethylsiloxane). *Analytical chemistry*, 70(23), 4974-4984.
- Eisenbach (1999)*: Mammalian sperm chemotaxis and its association with capacitation. *Developmental genetics*, 25(2), 87-94.
- Eisenbach and Giojalas (2006)*: Sperm guidance in mammals—an unpaved road to the egg. *Nature reviews Molecular cell biology*, 7(4), 276-285.
- El-Sherry, Elsayed Abdelhafez and Abdelgawad (2014)*: Characterization of rheotaxis of bull sperm using microfluidics. *Integrative Biology*, 6(12), 1111-1121.
- El-sherry, Abdel-Ghani, Abou-Khalil, Elsayed and Abdelgawad (2017)*: Effect of pH on rheotaxis of bull sperm using microfluidics. *Reproduction in Domestic Animals*, 52(5), 781-790.
- Elsayed, El-Sherry and Abdelgawad (2015)*: Development of computer-assisted sperm analysis plugin for analyzing sperm motion in microfluidic environments using Image-J. *Theriogenology*, 84(8), 1367-1377.
- Giojalas and Roasio (1998)*: Mouse spermatozoa modify their motility parameters and chemotactic response to factors from the oocyte microenvironment. *international journal of andrology*, 21(4), 201-206.
- Haubert, Drier and Beebe (2006)*: PDMS bonding by means of a portable, low-cost corona system. *Lab on a Chip*, 6(12), 1548-1549.
- Ishikawa, Usui, Yamashita, Kanemori and Baba (2016)*: Surfing and

- swimming of ejaculated sperm in the mouse oviduct. *Biology of reproduction*, 94(4), 89, 81-89.
- June Mullins and Saacke (1989): Study of the functional anatomy of bovine cervical mucosa with special reference to mucus secretion and sperm transport. *The Anatomical Record*, 225(2), 106-117.
- Kölle (2015): Transport, distribution and elimination of mammalian sperm following natural mating and insemination. *Reproduction in Domestic Animals*, 50, 2-6.
- Mathijssen, Shendruk, Yeomans and Doostmohammadi (2016): Upstream swimming in microbiological flows. *Physical Review Letters*, 116(2), 028104.
- Medeiros, Forell, Oliveira and Rodrigues (2002): Current status of sperm cryopreservation: why isn't it better? *Theriogenology*, 57(1), 327-344.
- Miki and Clapham (2013): Rheotaxis guides mammalian sperm. *Current Biology*, 23(6), 443-452.
- Morrell and Rodriguez-Martinez (2011): Practical applications of sperm selection techniques as a tool for improving reproductive efficiency. *Veterinary medicine international*, 2011.
- Moscovici, Chien, Abdelgawad and Sun (2010): Electrical power free, low dead volume, pressure-driven pumping for microfluidic applications. *Biomicrofluidics*, 4(4), 046501.
- Munson, Young and Okiishi (2002): Fundamentals of Fluids Mechanics, Edisi 4, Jhon Wiley & Sons. Inc, New York.
- Nasser, Fath El-Bab, Abdel-Mawgood, Mohamed, and Saleh (2019): CO2 laser fabrication of PMMA microfluidic double T-junction device with modified inlet-angle for cost-effective PCR application. *Micromachines*, 10 (10), 678.
- Nishina, Matsuura and Naruse (2019): Spiral trajectory modulation of rheotactic motile human sperm in cylindrical microfluidic channels of different inner diameters. *Acta Medica Okayama*, 73(3), 213-221.
- O'Hanlon, Moench and Cone (2013): Vaginal pH and microbicidal lactic acid when lactobacilli dominate the microbiota. *PloS one*, 8(11), e80074.
- Pérez-Cerezales, Boryshpolets and Eisenbach. (2015): Behavioral mechanisms of mammalian sperm guidance. *Asian journal of andrology*, 17(4), 628.
- Rappa, Samargia, Sher, Pino, Rodriguez and Asghar (2018): Quantitative analysis of sperm rheotaxis using a microfluidic device. *Microfluidics and nanofluidics*, 22(9), 100.
- Romero-Aguirregomezcorta, Laguna-Barraza, Fernández-González, Štiavnická, Ward, Cloherty and Gutiérrez-Adán (2021): Sperm selection by rheotaxis improves sperm quality and early embryo development. *Reproduction*, 161(3), 343-352.
- Sarbandi, Lesani, Moghimi Zand and Nosrati (2021): Rheotaxis-based sperm separation using a biomimicry microfluidic device. *Scientific reports*, 11(1), 18327.
- Shah, and AL (1978): Laminar flow forced convection in ducts. A source book compact heat exchanger analytical data.
- Sharma, Kabir and Asghar (2022): Selection of healthy sperm based on positive rheotaxis using a microfluidic device. *Analyst*, 147(8), 1589-1597.
- Soler, Picazo-Bueno, Micó, Valverde, Bompert, Blasco and García-Molina (2018): Effect of counting

- chamber depth on the accuracy of lensless microscopy for the assessment of boar sperm motility. *Reproduction, fertility and development*, 30(6), 924-934.
- Suarez (2002)*: Formation of a reservoir of sperm in the oviduct. *Reproduction in Domestic Animals*, 37(3), 140-143.
- Suarez (2006)*: Interactions of spermatozoa with the female reproductive tract: inspiration for assisted reproduction. *Reproduction, fertility and development*, 19(1), 103-110.
- Suarez and Pacey (2006)*: Sperm transport in the female reproductive tract. *Human reproduction update*, 12(1), 23-37.
- Suarez, Susan and Lefebvre (1997)*: Distribution of mucus and sperm in bovine oviducts after artificial insemination: the physical environment of the oviductal sperm reservoir. *Biology of reproduction*, 56(2), 447-453.
- Wigby, Suarez, Lazzaro, Pizzari and Wolfner (2019)*: Sperm success and immunity. *Current topics in developmental biology*, 135, 287-313.
- Yániz, Lopez-Gatius, Santolaria and Mullins (2000)*: Study of the functional anatomy of bovine oviductal mucosa. *The Anatomical Record: An Official Publication of the American Association of Anatomists*, 260(3), 268-278.
- Zhang, Liu, Meriano, Ru, Xie, Luo and Sun (2016)*: Human sperm rheotaxis: a passive physical process. *Scientific reports*, 6(1), 23553.

## الانجذاب التياراتى ومعاملات الحركة للحيوانات المنوية فى طلائق الابغار داخل القنوات الدقيقة ذات الارتفاعات المختلفة

هيثم عبد العليم مفضل ، حسن عبد الصبور حسين ، أحمد محمد رشاد فتح الباب ،  
تيمور محمد الشرى

Email: [aboharona34@gmail.com](mailto:aboharona34@gmail.com) Assiut University web-site: [www.aun.edu.eg](http://www.aun.edu.eg)

فى الأونة الأخيرة ، جذبت الموائع الدقيقة الكثير من الاهتمام فى التكاثر بسبب قدرتها على محاكاة البيئة الطبيعية داخل الجهاز التناسلى الأنثوى وقدرتها على فصل خلايا الحيوانات المنوية عالية الجودة باستخدام التأثير التياراتى كآلية اختيار. يشير التأثير التياراتى الموجب إلى قدرة الحيوانات المنوية على توجيه نفسها والسباحة ضد التيار السائل أثناء رحلة الإخصاب. فى هذه الدراسة ، قمنا بدراسة تأثير ارتفاعات القنوات الدقيقة المختلفة على الانجذاب التياراتى الإيجابى للحيوانات المنوية وحركية الحيوانات المنوية. استخدمنا قناتين صغيرتين بنفس العرض (٢٠٠ ميكرومتر) وارتفاعات مختلفة (القناة ١ = ارتفاع ٢٠ ميكرومتر والقناة ٢ = ارتفاع ١٠٠ ميكرومتر). تم الحصول على عينات الحيوانات المنوية من ثيران معروفة الخصوبة وتم تحليلها باستخدام نظام تحليل الحيوانات المنوية بمساعدة الكمبيوتر. أظهرت النتائج أن التأثير التياراتى الموجب وجميع حركات الحيوانات المنوية والتي تشمل السرعة المنحنية وسرعة الخط المستقيم ومتوسط سرعة المسار ومعدل تردد الضربات للحيوانات المنوية، باستثناء الخطية ، كانت أعلى بشكل ملحوظ فى القناة ٢ ذات الارتفاع الأكبر (١٠٠ ميكرومتر) منها فى القناة ١ ذات الارتفاع المنخفض (٢٠ ميكرومتر). تشير النتائج التي توصلنا إليها إلى أن نسبة الانجذاب التياراتى الإيجابى للحيوانات المنوية والقيم الحركية للحيوانات المنوية داخل القنوات الدقيقة تعتمد بشكل أساسى على أبعاد القناة الدقيقة، والتي لها تأثير مباشر على توزيع السرعة داخل القناة. قد تكون هذه النتائج مفيدة لتطوير الأجهزة المستخدمة فى فصل واختيار الحيوانات المنوية فى المستقبل.